RSC Advances

ROYAL SOCIETY OF CHEMISTRY

www.rsc.org/advances

Octreotide Acetate-templated Self-Assembly Pt Nanoparticles and Their Anti-tumor Efficacy

Weili Xue, Xiaoning Zhao, Dawei Gao*, Faming Gao*, Zi Wang, Yanping Liu, Xuwu Zhang, Liyao Luo, Zhiwei Liu

Applying Chemistry Key Lab of Hebei Province, Yanshan University, No.438 Hebei Street, Qinhuangdao, 066004, China.

Tel: +86 335 8387553;

Fax: +86 335 8061569

Correspondence should be addressed to Dawei Gao; dwgao@ysu.edu.cn and Faming Gao; fmgao@ysu.edu.cn

Weili Xue and Xiaoning Zhao have same contribution for the paper.

Octreotide Acetate-templated Self-Assembly Pt Nanoparticles and Their Anti-tumor Efficacy

Abstract The platinum nanoparticles (PtNPs) were assembled in the chain-like structure by activating chemical groups of the octreotide acetate (AOC) template. Tumor-bearing mice were inoculated with cervical carcinoma cells, and then treated with low dose of AOC-PtNPs (AOC-PtNPs-L), high dose of AOC-PtNPs (AOC-PtNPs-H), sterile physiological saline and cyclophosphamide, respectively. The results suggested that tumor inhibition rates of cyclophosphamide, AOC-PtNPs-L and AOC-PtNPs-H were 87.0%, 38.3% and 42.5%; and the apoptosis rates of the tumor-bearing mice were 30.95%, 23.41% and 26.64%, respectively. More importantly, the histopathological study results implied that AOC-PtNPs had no toxicity or side-effects on liver and kidney tissues, but obvious inhibitory effects on tumors. In addition, MTT assay results showed that as-prepared AOC-PtNPs had higher inhibition rate on Hela cells than those of single AOC or PtNPs. Therefore, AOC-PtNPs have great potentials as antitumor drugs for cancer therapy in future.

Keywords: Octreotide acetate (AOC), Pt nanoparticles (PtNPs), Bio-template, Tumor inhibition, Cervical carcinoma

Introduction

Cervical carcinoma, which is one of the main causes of cancer-related deaths in females, arouses great concern, which also is the second most common cancer among women. Approximately 83% of the cases occur in developing countries, especially in South America, Asia and Africa, accounting for 15% of all cancers in women.[1] So far, most treatments of cervical cancer derive from studies including surgery, radiation and chemotherapy. Among the above therapeutics, chemotherapy is a foremost remedial approach for the treatment of localized and metastasized tumors.[2] For chemotherapy, agents such as doxorubicin, cyclophosphamide or combination drugs have been widely used in cervical carcinoma treatment and they ultimately improve quality of life.[3] However, these agents also show unexpected toxicity and serious side-effects. A main obstacle for successful chemotherapy is the resistance of cancer cells to therapeutic drugs and the destructive actions of these drugs to normal cells, tissues, and organs.[4]

Platinum compounds such as cisplatin and carboplatin have found wide application in cancer chemotherapy.[5, 6] Also other platinum compounds are under investigation for anti-cancer treatment, such as ormaplatin and oxaliplatin.[7] In addition to platinum compounds, derivatives of other metals are being investigated for their anti-tumor properties e.g. titanocene.[8] Cisplatin is used in the treatment of a number of cancers, but its applicability is still limited to a relatively narrow range of tumors. In comparison to cisplatin, carboplatin has lower toxicity which has been the advantage that enabled it to achieve worldwide approval and use. Unfortunately, carboplatin is still only active in the same range of tumors as cisplatin and is still administered intravenously.

Currently, the cancer therapy has become a multidisciplinary challenge requiring close collaboration among clinicians, biological, materials scientists and chemistry. The ultimate goal of cancer therapeutics is to increase the survival time and the quality of life of the patient by reducing the systemic toxicity of chemotherapy.[9] At present, octreotide acetate has been used as an antitumor drug for clinic treatment.[10-12] Octreotide, as a hydrosoluble spheroprotein, is composed of eight amino acids, containing amines amidogen, hydroxyl disulfide bond, which is liable to combine with ions. Hence, octreotide template is prone to be combined with platinum to prepare nanoparticles.[13] Moreover, nano-sized platinum particles have multiple biomedical applications such as thermotherapy, radiation and catalyst. To our previous study, the combination of octreotide acetate with nano platinum particles is available.[14] In this study, we mainly

investigate the antitumor activity and cytotoxicity of the complex of octreotide acetate-templated Pt nanoparticles.

Materials and methods

Materials and animals

U14 cervical carcinoma cells were purchased from the Institute of Meteria Medica, Chinese Academy of Medical Sciences, and Peking Union Medical College. Kunming mice were purchased from the Laboratory Animal Center of the Academy of Military Medical Sciences (China).

Thirty-two healthy female Kunming mice (7–8 weeks), which were in good state and at similar weights (about 20 g), were fed for 7 days in a temperature-controlled mouse room. The mice were maintained under standard conditions of temperature (22–25 ^{o}C), a humidity of 60 ± 10% and a 12 h light/dark cycle. The animals were fed with a standard diet of mouse chow and water was allowed ad libitum. All experimental animal protocols were approved and in accordance with the Guide to the Care and Use of Experiment Animals (Canadian Council on Animal Care).

Preparation of AOC-PtNPs

The procedures of preparing AOC-PtNPs were the same as our previous work. 0.5 mg of AOC was dissolved in 1 mL of acidic solution (pH 2.0) to obtain 0.5 mM AOC acidic solution. Then, 200μL of the AOC acidic solution was mixed with a prepared aqueous solution of $PtCl_4$ (5 mM, 200 μL) and co-incubated in a shaking bath (13 ^{o}C, 130 rpm) for 24 h. Finally, the incubation solution was reduced by adding fresh DMAB solution (25 mM, 150 μL), drop by drop to prepare AOC-PtNPs. In the reduction process, the color of the solution was changed from faint yellow to grayish-black, and there was no precipitation in solution.

Characterization of AOC-PtNPs

Transmission electron microscopy (TEM)

The morphologies and sizes of the samples were observed on a TEM operated at 80 kV. TEM samples were prepared by placing drops of AOC-PtNPs suspension onto carbon-coated copper grids. To investigate the stability of as-prepared AOC-PtNPs, AOC-PtNPs suspension was centrifuged at 10000 rpm for 5 min and washed with double distilled water three times. Finally, the black precipitate was dissolved with double distilled water and carried out for a TEM test.

Particle size and zeta potential

Malvern Zetasizer ZS (Malvern Instruments, UK) was used to measure the sizes and surface zeta potentials of the prepared AOC-PtNPs. The mean diameters and zeta potentials of AOC-PtNPs were determined by dynamic light scattering (DLS) and electrophoretic mobility measurement, respectively. The zeta potentials of a AOC solution at pH 2 was also measured. All characterization measurements were repeated three times at 25 ^{o}C.

AOC loading on platinum nanoparticles

To investigate the loading efficiency and loading capacity of AOC on Pt nanoparticles, the prepared AOC-PtNPs solution was centrifuged at 12000 rpm for 10 min and washed with double distilled water two times in order to remove free AOC molecules. After that, the loading capacity and efficiency were evaluated by measuring the relative intensity of the UV−vis absorption of the standard AOC solution and supernatant at 277 nm, respectively.

U14 mouse cervical carcinoma-bearing solid tumor model

To investigate the anti-tumor efficacy of AOC-PtNPs in *vivo*, we established the cervical carcinoma xenograft animal model through transplantation of the U14 cells into female Kunming mice. Before the solid tumor model was established, all the tested mice were fasted and given free access to water for 12 h. The imbibed ascites from celiac tumor-bearing mice were diluted by sterile physiological saline (1:3, v / v). The density of the cell suspension was approximately adjusted to 2×10^{6} mL^{-1}. All these procedures were performed in sterile conditions. Then U14 mouse cervical carcinoma cells were transplanted subcutaneously into the oxter of the right forelimb of the mice. The successful ratio of cell inoculation in the experiment was up to 100%. Various drugs in different doses were offered to mice after 24 h of inoculating tumor cells.

Groups and treatment scheme of experimental animals

The mice were evenly divided into 4 groups randomly with each group of 8 mice. Mice in each group were marked after being weighed. The treatment methods for each group were as following description. Mice in the negative control (NC) group were injected intraperitoneally with sterile physiological saline; the mice in the positive control (PC) group were injected intraperitoneally with 5 mg mL^{-1} cyclophosphamide solution once a day for a total of 10 days; Mice in the AOC-PtNPs-L group and AOC-PtNPs-H groups were injected intraperitoneally with 0.3 and 0.6 mg mL^{-1} AOC-PtNPs solution once a day for a total of 10 days, respectively.

Effects of AOC-PtNPs on body weight of mice

The mouse body weight was monitored every day after drug treatment. Ten days later, all of the mice treated with aether anesthesia were sacrificed. The tissues (liver, kidney and tumors) were removed and flushed with 0.9% NaCl (w=v) three times to thoroughly remove the remaining blood.[15] Afterwards, all the tissues were weighed separately and stored in formalin.

Determination of tumor inhibition rate

The tumor tissues were removed and weighed after visual inspection. The tumor inhibition rate was calculated accordingly. Tumor inhibition rate = (mean tumor weight of NC − mean tumor weight of treatment group) / mean tumor weight of NC × 100%.

Annexin V-FITC / PI double staining assay

To understand the specific mechanism of underlying the enhanced anti-tumor efficacy of AOC-PtNPs, cell apoptosis was further analyzed using FCM. Apoptosis was detected by staining with annexin V and PI labeling, since annexin V could identify the externalization of phosphatidylserine during the apoptosis process.[16] A series of morphology changes can be observed in the apoptosis procedure, and transformation of the cell membrane is one of the characteristics in the earlier stages. An annexin V-FITC/PI kit was chosen to determine the percentage of apoptosis. The cells were collected by centrifugation and stained for 5 min at room temperature with annexin V-FITC/PI double staining. The cells were then analyzed by the flow cytometer (Beckman Coulter) using the manufacturer's analysis software. Approximately 10 000 counts were made for each sample.

Histopathological study

The liver, kidney and tumor tissues were carefully removed and fixed in 10% neutral buffered formalin for 24 h. All tissues were dehydrated in a series of ethanol, cleared in xylene and embedded in paraffin wax. Sections of 3–5 μm thickness were obtained using a rotator microtome (Leica Company, Germany). The sections attained were stretched on slides, subjected to paraffin removal and rehydrated in a regressive series of ethanol and stained with hematoxylin eosin.[17] It is important to point out that all glass slides used in experiments were pretreated with poly-L-lysine solution or APES so that sections could adhere to the slides tightly. All sections were observed with a light microscope and photographed for histological examination.

MTT assay

The classical MTT method was utilized to detect the inhibition effects of the prepared AOC-PtNPs on Hela cells in *vitro*. For comparison, single AOC and PtNPs served as the control groups. In this study, PtNPs were obtained by ultracentrifugation of AOC-PtNPs at 41000 rpm for 1 h, not simply reducing $PtCl_4$ solution with $NaBH_4$. The above samples were filtered through sterile 0.22 μm filter membrane, and then they were diluted with phosphate-buffered saline to obtain various concentrations of drugs (10 μg mL^{-1}, 50 μg mL^{-1} and 100 μg mL^{-1}).

Briefly, Hela cells were grown in DMEM medium with 10% fetal bovine serum under sterile conditions with 5% of CO_2 at 37 ^{o}C, and according to the growth conditions of cells, subcultures were carried out at intervals of 2–3 days. Ultimately, Hela cells in the logarithmic phase were used for the following MTT assay. Adequate numbers of cells were plated in each well of a 96-well plate in 0.1 mL of complete culture medium and allowed to attach for 24 h. After that, each sample was done in triplicate (100 μL per well)

into the appropriate well of culture dish. The drug-treated cells were incubated for 24 hours under the conditions mentioned above, and inhibition effect of each sample on Hela cells was analyzed using the MTT agent. 24 hours later, the medium was discarded and the cells were incubated with 200 μL fresh medium containing 0.5 mg mL^{-1} MTT for 4 hours. After removing the unreduced MTT, 150 μL of DMSO was added to each well to dissolve the formazan crystals. Finally, the absorbance of samples was measured by an ELISA reader (MK3, Thermo Co., USA) at 570 nm.

Statistical analysis

All the obtained data are expressed as mean ± standard error unless particularly outlined. Origin software (version7.0) was utilized to deal with numeric plots. SPSS statistical software (version 13.0) was performed for statistical analysis. Statistical significance was assessed by a one-way analysis of variance test. Differences were considered statistically significant if P was <0.05.

Results and discussion

Morphological analysis of prepared AOC-PtNPs

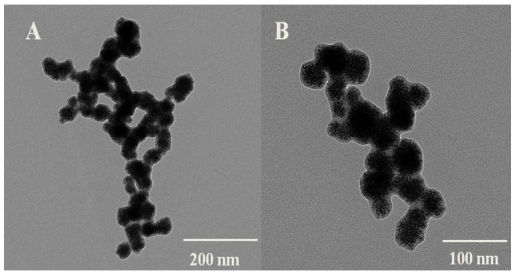

Fig. 1 TEM images of platinum nanochains produced using AOC as bio-template at pH 2.0 (A, unwashed; B, washed)

From Fig. 1, chain-like structure of as-prepared AOC-PtNPs can be clearly seen. There is a uniform distribution of the particles along the Pt nanochains. Almost all the AOC were combined with the Pt particles, and no loose particles could be found, which indicates that the AOC molecules were used effectively to mostly form spheroidal Pt nanochains. In addition, the morphology of the sample washed by double distilled water was still chain-like structure, and there was no seperation between Pt particles and AOC. Therefore, it can be concluded that the prepared AOC-PtNPs was stable in neutral condition.

Particle size and zeta potential

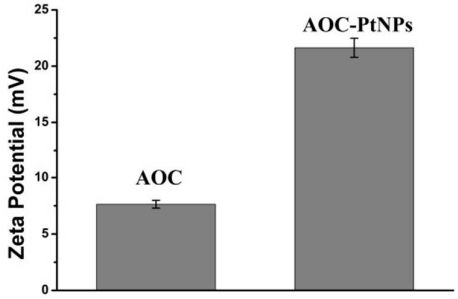

Fig. 2 Surface zeta potentials of AOC and AOC-PtNPs. Data represent mean ± SE (n=3).

In this study, the zeta potentials were determined by electrophoretic mobility measurement. The surface zeta potentials of single AOC solution (pH 2) and prepared AOC-PtNPs can be seen from fig. 2. The single AOC solution at pH2 had a marked positive charges (7.64 ± 0.34 mV), which contributed to combining Pt complex ion which had negative charges. The surface zeta potential of the prepared AOC-PtNPs was 21.63 ± 0.85 mV, indicating AOC molecules aggregated during the process of forming AOC-PtNPs. Positively charged AOC-PtNPs can be combined with the negative charges on the surface of the tumor cells. Hence, the prepared AOC-PtNPs tend to aggregate in the tumor cells and cause cell uptake, which can inhibit effectively the growth of tumor cells.

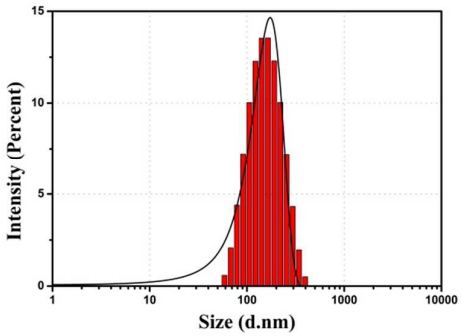

Fig. 3 Size distribution of as-prepared AOC-PtNPs with the log-normal fitting curve

The particle sizes were detected by the DLS. The size distribution with the log-normal fitting curve of the prepared AOC-PtNPs was shown in Fig. 3. The average diameter of AOC-PtNPs was around 174.18 nm. The result also indicated that the particle sizes of

the prepared AOC-PtNPs were relatively uniform.

Loading efficiency and loading capacity of AOC on PtNPs

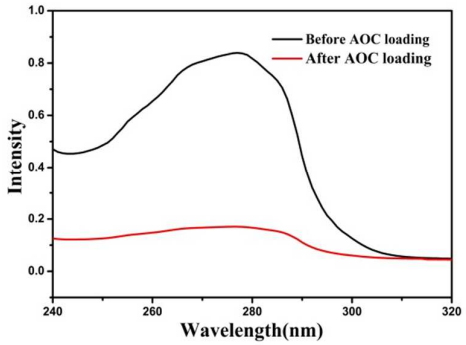

Fig. 4 UV−vis absorption spectra of standard AOC solution before and after loading on Pt nanoparticles

As shown in fig. 4, there is a significant reduction of the absorption intensity, indicating that the AOC has a good ability in loading on the platinum nanoparticles. The loading efficiency of the AOC on platinum particles is 79.7%, and the loading capacity is 408.7 mg of AOC/g of platinum nanoparticles.

Effects of AOC-PtNPs on body weight of mice

The mouse body weights were monitored throughout the test period as an indication of effects of the drugs. In the whole experiment process, all the mice were in favorable condition; body weight increased reposefully, and there was no death.

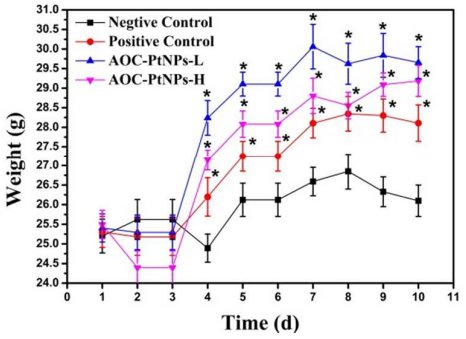

Fig.5 Trends in body weight of mice during therapy process (Values are expressed as mean ± SE of 8 mice per group; * indicates $P < 0.05$ compared with NC group)

The results shown as Fig. 5 suggested that the body weight of mice in NC group was significantly lower than other groups. Thus it can be seen that physiological saline had no inhibiting effect on tumor, and the tumor had a great influence on health status. However, the mice in PC group grew normally and the increase of body weight was obvious.

Though body weights of mice in drug treated groups decreased on the second day, the entire trends of their body weights were increasing. Therefore cyclophosphamide, AOC-PtNPs-L and AOC-PtNPs-H all had significant inhibiting effects on tumor.

Inhibition effect of AOC-PtNPs on U14 cervical cancer solid tumor

After 10 days of drug treatment, it was observed that cyclophosphamide, AOC-PtNPs-L and AOC-PtNPs-H all exhibited pronounced inhibitory effect on transplanted tumors. The results were shown as Table 2.

Table 2 Inhibition effect of AOC-PtNPs on U14 cervical cancer solid tumor of mice

Groups	Tumor weight (g)	Inhibition rate (%)
NC	1.48 ± 0.11	-
PC	0.19 ± 0.01*	87.0*
AOC-PtNPs-L	0.91 ± 0.02*#	38.3* #
AOC-PtNPs-H	0.84 ± 0.06*#	42.5* #

Note: Values are expressed as mean ± SE of 8 mice per group. NC, negative control group; PC, positive control group; AOC-PtNPs-L, mice treated with low dose of AOC-PtNPs; AOC-PtNPs-H, mice treated with high dose of AOC-PtNPs. * indicates $P < 0.05$ compared with NC group; # indicates $P < 0.01$ compared with PC group.

All data obtained were analyzed by one-way ANOVA; the results showed that mean tumor weights of treatment groups were notably lower than that of NC. The mean tumor weight of NC was 1.48 ± 0.11 g, whereas the values of AOC-PtNPs-L, AOC-PtNPs-H and PC groups were only 0.91 ± 0.02 g, 0.84±0.06 and 0.19 ± 0.01 g, and inhibition rates were 38.3%, 42.5% and 87.97% respectively (table 1). Mean tumor weights of AOC-PtNPs-L and AOC-PtNPs-H showed significant differences ($P < 0.05$) compared with NC. The results demonstrated that AOC-PtNPs suppressed U14 tumor growth prominently, and there were significant dose-dependent effects on tumor weights by AOC-PtNPs treatment.

Measurement of apoptosis using FCM

Flow cytometry (FCM) can be used to analyze quantitatively and screen unicellular creatures and

other biological particles at a functional level. There are many advantages in applications of FCM, such as rapid speed precision, great accuracy and so on. Especially when it is used in the process of apoptosis, the detection accuracy of FCM is remarkable.[18] In the measurement with annexin V, the kit can distinguish its union with annexin and PI: cell necrosis (cell death independent of apoptosis), located upper left (annexin V/PI =－ / ＋); necrotic and late apoptotic cells, (annexin V/PI=＋ / ＋) upper right; viable cells, lower left (annexin V/PI =－ / －) apoptotic cells in the early stage, lower right (annexin V/PI=＋ / －).

In the experiment with annexin V-FITC, there were significant differences (P < 0.05) in viability, apoptosis and necrosis with cyclophosphamide, AOC-PtNPs-L and AOC-PtNPs-H (Fig. 6).

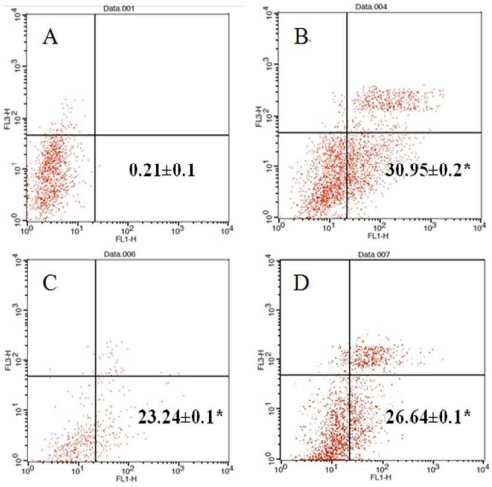

Fig. 6 Flow cytometry studies of apoptosis for each sample (A) Negative control (NC); (B) Positive control (PC); (C) AOC-PtNPs-L; (D) AOC-PtNPs-H

Apoptosis rates of tumor cells of tested mice in treatment groups were 30.95%, 23.41% and 26.64% respectively. The result suggested that apoptosis rates of PC were obviously higher than that of AOC-PtNPs, and it was presumable that both cyclophosphamide and AOC-PtNPs presented inhibitory effects on tumor growth; meanwhile, the effects of inducing apoptosis were distinct. Furthermore, a prominent increase was observed in AOC-PtNPs-H group compared with AOC-PtNPs-L group. Therefore, it was indicated that anti-tumor activity of AOC-PtNPs was remarkable.

Effects of AOC-PtNPs on histopathology of the tumor bearing mice

Effects of AOC-PtNPs on the kidney tissue structure of mice

The kidney tissues were immediately removed after mice were sacrificed. It was observed that the color, gloss and texture of kidney were normal in AOC-PtNPs-L and AOC-PtNPs-H. No histopathological changes were discovered in the sections of kidney. As shown in Fig. 7, the structure of the kidney tubules was very clear, and the shape of the glomerulus was quite regular. Moreover, nephrocytes were arranged closely. It was indicated that AOC-PtNPs had no kidney injury.

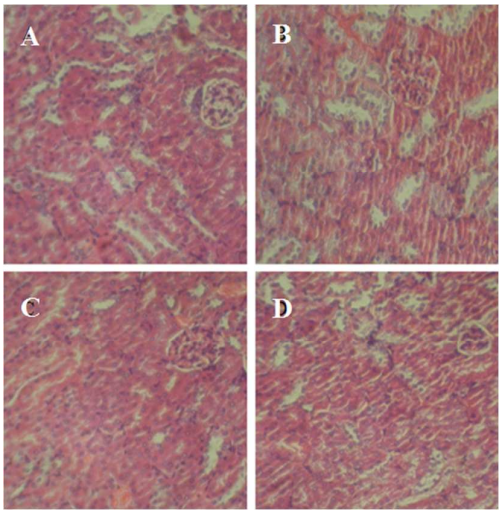

Fig. 7 Histological sections of the kidney tissue for: (A) negative control; (B) positive control; (C) AOC-PtNPs-L; (D) AOC-PtNPs-H.

Effects of AOC-PtNPs on the liver tissue structure of mice

Histopathologically, the same normal phenomena were observed from the color and texture of liver in AOC-PtNPs-L and AOC-PtNPs-H groups. No histopathological alterations of liver tissue were observed. As shown in Fig. 8, hepatocytes were arranged closely and regularly. The volume of hepatic cells was normal and no dropsy was noted. Furthermore, the nucleolus was clear, and the central veins and hepatic lobule were obviously seen as well. It was indicated that both AOC-PtNPs-L and AOC-PtNPs-H didn't cause damage on livers of mice.

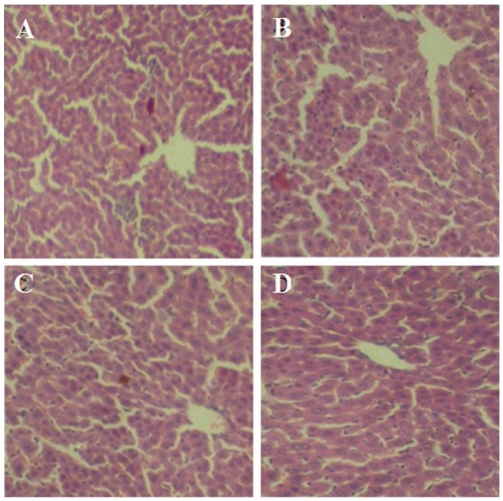

Fig. 8 Histological sections of the liver tissue for: (A) negative control; (B) positive control; (C) AOC-PtNPs-L; (D) AOC-PtNPs-H.

Effects of AOC-PtNPs on the tumor tissue structure of mice

The tumor tissues dissected in NC mice were fluidified severely, and adjacent to pleura. Some tumor tissues even invaded the skeletal muscles, and represented diffusible growth and abundant blood vessels. Based on the comparison of those in NC mice, tumor tissues in other groups showed a clear borderline with other body parts. No invasion of skeletal muscle was observed; tumor tissues could be easily dissected. The tumor body was tight and firm, the color was white and blood vessels were not rich. In addition, tumor weight in treatment groups was lower than that of NC, according to the tumor weight of experimental mice.

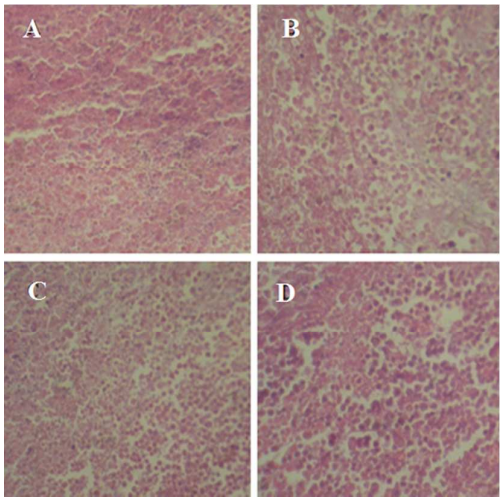

Fig. 9 Histological sections of the tumor tissue for: (A) negative control; (B) Positive control; (C) AOC-PtNPs-L; (D) AOC-PtNPs-H

Histological sections of the tumor tissue were shown in Fig. 9, and the tumor cells in NC were round or polygonal. The nucleolus was round or elliptic and mostly very large, and the nuclear envelope was clear. Rough chromatin and little cytoplasm were shown to be prominent. The number of tumor cells in AOC-PtNPs-H decreased obviously compared with that of NC. Malignant tumor cells presented heteromorphosis; apoptosis of many single dispersive tumor cells and tumor necrosis were seen. The adhesion of tumor cells was poor. It was also found that monolayer and necrotic cells appeared in tumor tissues of mice treated with AOC-PtNPs and cyclophosphamide. The results demonstrated AOC-PtNPs had anti-tumor activity indeed.

Antitumor efficacy of AOC-PtNPs on Hela cells in vitro

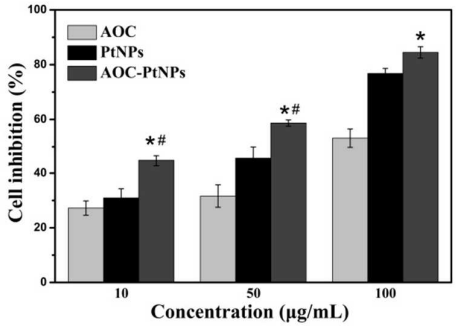

Fig. 10 Inhibition effects of AOC, PtNPs and AOC-PtNPs on Hela cells. All values are expressed as mean ± SE (n=3). (* indicates $P < 0.05$ compared with AOC; # indicates $P < 0.05$ compared with PtNPs)

From fig. 10, it can be seen that all the samples show significant inhibition effects on Hela cells with their concentrations increasing. At 10 μg mL^{-1}, inhibition rates had no significant difference between AOC and PtNPs, which were 27.23% and 31.63%, respectively. However, with the concentrations increasing, inhibition rates of PtNPs were significantly higher than those of AOC though the inhibition rate of AOC also increased obviously. To sum up, inhibition rates of AOC-PtNPs on Hela cells were higher than those of single AOC and PtNPs at any concentration. The results implied that the antitumor efficacy of single AOC and PtNPs can be enhanced when they combined into AOC-PtNPs.

Discussion

Platinum, as a kind of noble metal, exhibits special

efficacy particularly in cancer therapy when its size reaches nanometer grade.[19] In the case of the antitumor mechanism of PtNPs, earlier reports have emphasized that PtNPs inside the cell can be hydrolyzed to release Pt^{2+}, which could block cell division by binding to DNA.[20] We speculate the involvement of an analogous mechanism in PtNPs toxicity wherein released Pt^{2+} ions might halt DNA synthesis. In this sense, PtNPs can interact with DNA to produce Pt-DNA adducts through hydrolyzation.

The synthetic somatostatin analogue octreotide has been tested for efficacy in various solid tumours, including breast, prostate, colon, pancreas, and small cell lung carcinoma.[21] Though the exact mechanism of the antitumor effect of octreotide on carcinoma described above has not been elucidated, octreotide has been suggested to be mediated by inhibiting endothelial cells proliferation, invasion and differentiation, and the production of vascular endothelial growth factor in tumor cells.[22-24]

According to the finding of our experiment, the combination of octreotide with PtNPs has been shown to induce apoptosis in Hela cells, indicating that the linkage of PtNPs to octreotide does not change the active center of the octreotide. In relation to antitumor mechanism of AOC-PtNPs on cervical carcinoma, at the same time as octreotide inhibits the growth of Hela cells, Pt(0) on the surface of octreotide can be hydrolyzed to release Pt^{2+}, which interacts with DNA to form Pt-DNA adducts, thereby blocking fundamental cellular processes.

However, the tumor inhibition rate of AOC-PtNPs is lower than that of PC group, which is consistent with the dose-dependent property of AOC-PtNPs. By comparing the treatment scheme of experimental animals, it can be seen that the dosage of PC group is 5 mg mL^{-1}, higher than 8 times as many as that of AOC-PtNPs-H group and 16 times as many as that of AOC-PtNPs-L group, on the premise that the total volume of each group is equal. Nonetheless, the tumor inhibition rate of PC group is approximately only twice higher than that of AOC-PtNPs group. Comparing AOC-PtNPs-H group with AOC-PtNPs-L group, the dosage of the former is twice as many as that of the later, and the tumor inhibition rate is increased by 4.2%. Therefore, it was indicated that anti-tumor activity of AOC-PtNPs was remarkable.

Histopathological studies have been utilized to help establish causal relationships between contaminant exposure and various biological responses.[25] The paraffin methodology requires less specified equipment and could supply high quality slides adequate for many purposes.[26] Our histopathological results indicate that no changes of liver or kidney tissues take place after treatment with AOC-PtNPs. The histopathological sections of tumor tissues in tested groups demonstrate that AOC-PtNPs has strong inhibitory effects on transplanted U14 cells. Our present investigations clearly reveal that AOC-PtNPs would serve as anti-tumor drugs for future tumor therapy.

Conclusions

According to the results, AOC templated Pt nanoparticles via injection significantly suppressed tumor growth compared with NC group. In particular, a high dose of AOC-PtNPs remarkably enhanced the inhibitory ratio of tumor cells. Flow cytometry analysis revealed that high dose and low dose of AOC-PtNPs suppressed tumor growth through induction of apoptosis. Furthermore, high dose of AOC-PtNPs showed higher apoptosis ratio. In addition, the findings from the histopathological observations implied that AOC-PtNPs had no toxicity or side-effects on liver and kidney tissues, which also indicated that AOC-PtNPs had an inhibitory effect on tumors, and the inhibition action of high dose of AOC-PtNPs was particularly evident. MTT assay results suggested that cell inhibition effects of AOC-PtNPs on Hela cells were significantly stronger than those of single AOC or PtNPs. Therefore, this study can provide a basis for the further investigation on the anti-tumor activity of AOC-PtNPs formulation.

Acknowledgments

This work was financially supported by a research fund from the National Natural Science Foundation (No. 21476190), Hebei Province Key Basic Research Foundation (No.15961301D) and Qinhuangdao Science and technology research and development

Project (No. 201202B029).

Reference

1. D. M. Parkin, F. Bray, J. Ferlay and P. Pisani, *CA: a cancer journal for clinicians*, 2005, 55, 74-108.
2. A. Jain, K. Jain, P. Kesharwani and N. K. Jain, *Journal of nanoparticle research*, 2013, 15, 1-38.
3. J. Tang, Y. Tang, J. Yang and S. Huang, *Gynecologic oncology*, 2012, 125, 297-302.
4. N. Kasoju, D. K. Bora, R. R. Bhonde and U. Bora, *Journal of Nanoparticle Research*, 2010, 12, 801-810.
5. P. G. Rose, B. N. Bundy, E. B. Watkins, J. T. Thigpen, G. Deppe, M. A. Maiman, D. L. Clarke-Pearson and S. Insalaco, *New England Journal of Medicine*, 1999, 340, 1144-1153.
6. L. Murray, C. Bridgewater and D. Levy, *Clinical Oncology*, 2011, 23, 55-61.
7. O. GHIRARDI, P. L. GIUDICE, C. PISANO, M. VERTECHY, A. BELLUCCI, L. VESCI, S. CUNDARI, M. MILOSO, L. M. RIGAMONTI and G. NICOLINI, *Anticancer research*, 2005, 25, 2681-2687.
8. C. M. Kurbacher, H. W. Bruckner, P. E. Andreotti, J. A. Kurbacher, G. Sa and D. Krebs, *Anti-cancer drugs*, 1995, 6, 697.
9. J. D. Byrne, T. Betancourt and L. Brannon-Peppas, *Advanced drug delivery reviews*, 2008, 60, 1615-1626.
10. N. Cheung and S. C. Boyages, *Endocrinology*, 1995, 136, 4174-4181.
11. O. Nilsson, *British journal of cancer*, 1998, 77, 632.
12. M. Höcker and B. Wiedenmann, *Italian journal of gastroenterology and hepatology*, 1999, 31, S139-142.
13. M. Sarikaya, C. Tamerler, A. K.-Y. Jen, K. Schulten and F. Baneyx, *Nature materials*, 2003, 2, 577-585.
14. X. Zhao, D. Gao, F. Gao, N. Li, J. Zhou and J. Hao, *Journal of nanoparticle research*, 2013, 15, 1-7.
15. H. D. Han, A. Lee, C. K. Song, T. Hwang, H. Seong, C. O. Lee and B. C. Shin, *International journal of pharmaceutics*, 2006, 313, 181-188.
16. K. Urech, J. Scher, K. Hostanska and H. Becker, *Journal of pharmacy and pharmacology*, 2005, 57, 101-109.
17. J. Bancroft, A. Stevens and D. Turner, *the text*, 1996, 766.
18. J. W. Tung, K. Heydari, R. Tirouvanziam, B. Sahaf, D. R. Parks, L. A. Herzenberg and L. A. Herzenberg, *Clinics in laboratory medicine*, 2007, 27, 453-468.
19. Y. Teow and S. Valiyaveettil, *Nanoscale*, 2010, 2, 2607-2613.
20. J. Gao, G. Liang, B. Zhang, Y. Kuang, X. Zhang and B. Xu, *Journal of the American Chemical Society*, 2007, 129, 1428-1433.
21. K. Oberg, *Nature Reviews Endocrinology*, 2010, 6, 188-189.
22. R. Danesi, C. Agen, U. Benelli, A. Paolo, D. Nardini, G. Bocci, F. Basolo, A. Campagni and M. D. Tacca, *Clinical Cancer Research*, 1997, 3, 265-272.
23. A. Albini, T. Florio, D. Giunciuglio, L. Masiello, S. Carlone, A. Corsaro, S. Thellung, T. Cai, D. Noonan and G. Schettini, *The FASEB journal*, 1999, 13, 647-655.
24. S. Cascinu, E. Del Ferro, M. Ligi, M. P. Staccioli, P. Giordani, V. Catalano, R. Agostinelli, P. Muretto and G. Catalano, *Cancer investigation*, 2001, 19, 8-12.
25. H. Boran, E. Capkin, I. Altinok and E. Terzi, *Experimental and Toxicologic Pathology*, 2012, 64, 175-179.
26. S. Glasson, M. Chambers, W. Van Den Berg and C. Little, *Osteoarthritis and Cartilage*, 2010, 18, S17-S23.